Original Article
^{68}Ga-PSMA PET/CT in the evaluation of locally advanced and metastatic breast cancer, a single center experience

Sevastian Medina-Ornelas[1], Franciso García-Perez[1], Enrique Estrada-Lobato[2], Francisco Ochoa-Carrillo[3]

[1]Departament of Nuclear Medicine and Molecular Imaging, Instituto Nacional de Cancerología, Mexico City, Mexico; [2]Human Health Department International Atomic Energy Agency (IAEA), Viena, Austria; [3]Department of Surgery, Instituto Nacional de Cancerología, Mexico City, Mexico

Abstract: Current research indicates that prostate-specific membrane antigen (PSMA) is related to angiogenesis of many solid tumors including breast cancer (BC), our objective is evaluating PSMA expression in primary tumor and metastatic BC by Positron emission tomography/computed tomography (PET/CT). In this retrospective study twenty-one patients with BC included all molecular subtypes, was evaluated with ^{18}F-FDG-PET/CT imaging as stratification and ^{68}Ga-PSMA-PET/CT. Primary sites of BC was identifying in all patients with ^{18}F-FDG-PET/CT. We identified lymph node metastases in 17 patients (81%) and metastatic disease in 15 patients (71%). A total 127 lesions were detected by ^{18}F-FDG-PET/CT, 30 of which were in the breast, 31 axillary lymph-node metastases, 25 mediastinal lymph-node metastases, 15 distant non-bone metastases and 26 bone metastases. ^{68}Ga-PSMA-11-PET/CT showed lower detection-rate (DRs) than did ^{18}F-FDG-PET/CT in all patients with LUM-A and LUM-B HER2. All ^{18}F-FDG PET/CT positive lesions in patients TPN (local, lymph nodes, and metastatic lesions) showed ^{68}Ga-PSMA-PET/CT uptake (P<0.05). Sensitivities and specificities of 99.2% and 93.6% for ^{18}F-FDG-PET/CT and for ^{68}Ga-PSMA-11-PET/CT of 84% and 91.8% (P<0.05). Accuracy measured as AUC was 0.86-0.95 in ^{18}F-FDG-PET/CT and 0.74-0.94 for ^{68}Ga-PSMA-PET/CT (P<0.05). In Patient-Based analysis we found that patients triple-negative subtype (TPN) evaluated with ^{68}Ga-PSMA-PET/CT identified a higher number of positive patients than did LUM A. We conclude that a significicate DRs to imaging with ^{68}Ga-PSMA-PET/CT in the staging of locally advanced and metastatic BC with high rates in patients TPN, LUM B HER2^{+} and HER2 overexpression. We believe that concept of theranostics it may be considered as a potential diagnostic and therapeutic target.

Keywords: ^{68}Ga-PSMA, breast cancer, positron emission tomography computed tomography, theranostics

Introduction

The breast cancer (BC) in Mexico is the most common malignancy and cause of cancer death in women, according to most recent statistic among incidence 39.5 per 100,000 and mortality of 9.9 per 100,000 females annually even though the incidence of BC is rising in the last decades. Cancer staging is the most important aspect in the decision of a treatment and for deciding personal treatment strategies [1, 2]. Recent data estimated that approximately 70% of women with metastatic breast cancer (mBC) were diagnosed in early stages (I-III) and later developed distant recurrence [3].

Positron Emission Tomography/Computed Tomography (PET/CT) is one of the imaging modalities which become successful not just in the

staging of the disease, but in the therapeutic response evaluation. In initial evaluation in absence of signs or symptoms suggesting metastases PET/CT with the most widely used radiotracer is the ^{18}F-fluoro-deoxyglucose (^{18}F-FDG) is not recommend, some guidelines suggest as optional for evaluation of patients with stage IIIA and higher disease according to American Joint Committee on Cancer (AJCC) staging system [4, 5].

Selective inhibition of angiogenesis is a key strategy in BC. This process requires early identification when first-line therapy fails. Prostate-specific membrane antigen (PSMA) is a type II transmembrane glycoprotein which is first cloned in the human prostate parenchyma and exhibits folate hydrolase/glutamate carboxy-peptidase II enzymatic activity [6]. In the pros-

Table 1. Patient characteristics, n = 21

Characteristics	
Age median (range)	51 (33-69)
Clinical stage (n, %)	
IIIA	6 (28.5%)
IIIB	5 (23.8%)
IIIC	4 (19.2%)
IV	6 (28.5%)
Breast cancer subtype	
LUM A (n, %)	4, 19%
LUM B HER2⁻ (n, %)	4, 19%
LUM B HER-2⁺ (n, %)	2, 9.5%
HER-2 overexpression (n, %)	6, 28.5%
TPN (n, %)	5, 24%

Abbreviations: LUM = molecular subtypes of breast cancer including luminal A and luminal B; HER-2 = human epidermal growth factor receptor 2; TPN = triple negative breast cancer.

tate gland, PSMA is expressed at low levels in benign prostatic epithelium and upregulated in the majority of advanced prostatic malignancies especially in acinar adenocarcinoma [7, 8].

Current research indicates that PSMA is related to angiogenesis of many solid tumors including kidney cancer, colorectal cancer, glioblastoma, pancreatic cancer, lung cancer, and bladder cancer; however, studies are limited in the use of this agent in BC [9-13]. Therefore, the purpose of this study is to demonstrate PSMA expression in primary tumor and metastatic BC sites, and assess its potential use as theragnostic target, regardless of the hormonal status and histology.

Materials and methods

The present retrospective clinical study was conducted at nuclear medicine and molecular Imaging department in Instituto Nacional de Cancerologia, Mexico, between January 2015 and July 2017. All PET/CT examinations were performed in compliance with 1964 Declaration of Helsinki, and the responsible regulatory bodies in Mexico. All patients received ^{68}Ga-PSMA under the "compassionate use" clause of the Mexico. Written informed consent was obtained from each patient.

Synthesis of ^{68}Ga-PSMA-11

^{68}Ga (half-life 68 min; β+ 89%; Eβ+ max. 1.9 MeV) was obtained from a ^{68}Ge/^{68}Ga generator

(Isotope Technologies Garching). The synthesis of Glu-NH-CO-NH-Lys(Ahx)-N,N'-Bis[2-hydroxy-5-(carboxyethyl)-benzyl]ethylenediamine-N,N'-diacetic acid (*HBED-CC*) was obtained from ABX Advanced Biomedical Compounds, and HBED-CC was selected because of its lipophilic nature. The synthesis of ^{68}Ga-PSMA was carried out on an iQS ^{68}Ga Fluidic Labeling Module (Isotope Technologies Garching), 0.1-1 nmol of Glu-NH-CO-NHLys (Ahx)-HBED-CC were added in a volume of 100 μL to a mixture of 10 μL 2.1 M HEPES solution and 10 μL [^{68}Ga]Ga^{3+} eluate (50-100 MBq). The pH of the labeling solution was adjusted to 4.2. The reaction mixture was incubated at ambient temperature for 2 min. The radiochemical yield (RCY) was determined using RP-HPLC. The final product was formulated in isotonic phosphate-buffered saline (PBS) with subsequent sterile filtration. The radiolabelling and purification of the PSMA ligand was done using an automated module. The radiochemical purities of ^{68}Ga-PSMA were >98% and were analyzed using reversed-phase highperformance liquid chromatography (RP-HPLC; Chromolith RP-18e, 100 × 4.6 mm; Merck, Darmstadt, Germany).

Patients

Twenty-one patients (range 33-69 years, mean age 51 years) in our institution with BC were studied between January 2015 and July 2017. Four patients were luminal A (LUM-A); Four patients were LUM B HER2 positive (LUM-B HER2$^+$ [human epidermal growth factor receptor 2]); Two patients were LUM B HER2 negative (LUM-B HER2$^-$); Six patients were HER2 overexpression (HER2$^+$), and five patients were triple negative (TPN). Inclusion criteria for ^{68}Ga-PSMA-PET/CT were that these patients were diagnosed with metastatic-BC (*m*BC), and baseline ^{18}F-FDG-PET/CT imaging was acquired as stratification before initiate therapy (1-2 week's). In all patients, available imaging data performed as part of the staging. The most representative characteristics of the population study are resumed in **Table 1**. For validation of the metastases in lack of histological proof of bone metastases in all cases it was based on a consensus review of all available current and follow-up clinical data and imaging studies, all patients had a follow-up imaging modality available, confirming or ruling out bone metastases.
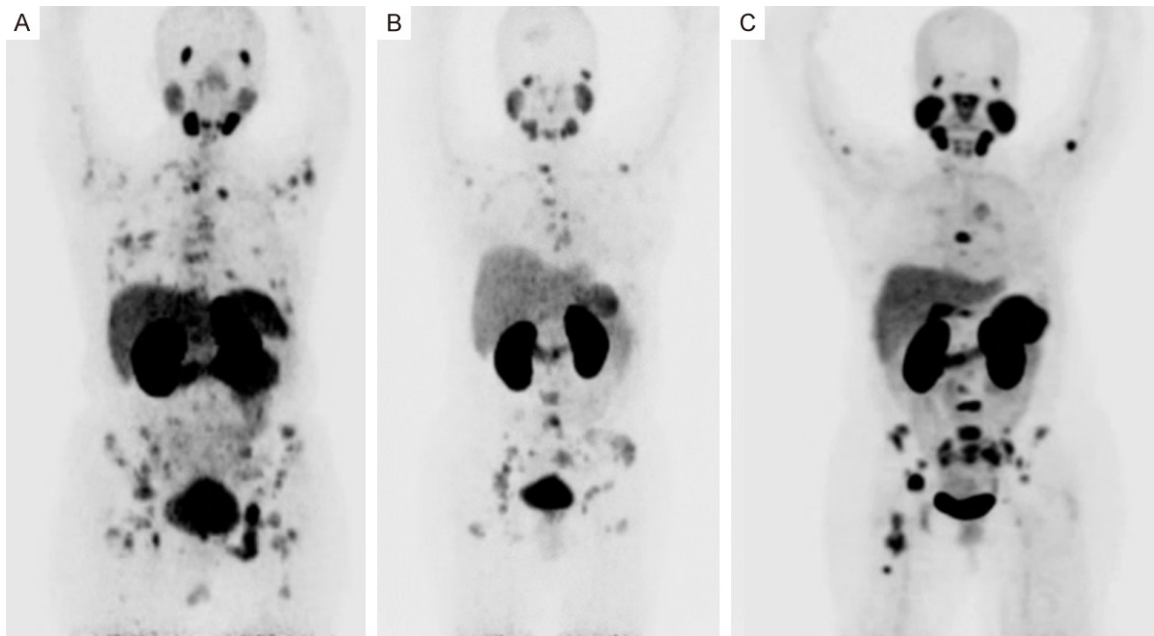
Figure 1. A. Maximal intensity projection (MIP) Positron Emission Tomography PET with 68Ga-PSMA in patient with TPN breast cancer, showed normal biodistribution and primary site in right breast, multiple bone and lymph-node metastases. B. MIP in patient with LUM-B HER2 positive breast cancer, showed multiple bone metastases with faint uptake in primary site in the left breast. C. MIP in patient with Her-2 overexpression breast cancer, showed multiple bone metastases with faint uptake in primary site in the right breast.

Imaging protocol

Imaging was performed with a Biograph mCT 20 PET/CT (Siemens Medical Solutions, USA) at the nuclear medicine and molecular Imaging department in Instituto Nacional de Cancerologia. The 68Ga-PSMA was applied to patients via an intravenous bolus (mean 6, SD 155.5, 6-27.4 MBq; range, 88-240 MBq). PET acquisition was started at a mean time of 59 ± 10.1 min after tracer injection (range, 49-70 min). Low-dose CT (from skull to mid-thigh) correction was performed for both attenuation correction and topographic localization. The CT parameters used for acquisition were 140 kV, 80 mA, and 0.5 s per rotation, with a pitch of 6:1 and a slice thickness of 5 mm. After completion of the CT scan, PET data were acquired for 3 min per bed position. Emission data were corrected for randoms, dead time, scatter, and attenuation and were reconstructed iteratively by an ordered-subsets expectation maximization algorithm (4 iterations, 8 subsets) followed by a post-reconstruction smoothing gaussian filter (5 mm in full width at one-half maximum).

Imaging analysis

PET/CT images in all standard planes were reviewed by use of the dedicated software (syngo by SIEMENS). Images were analyzed visually and quantitatively by two nuclear medicine physicians with more than 5 years of experience ($\kappa = 0.85$). Maximum standardized uptake values (SUVmax) were obtained by drawing circular regions of interest, which were automatically adapted (40% isocontour) to a 3D volume of interest (VOI) using syngo software. SUVmax was chosen due to its higher reproducibility between different investigators when compared to SUVmean and SUVmedian. In addition, dependent on the VOI's drawn by the investigators, whereas SUVmax is independent.

18F-FDG-PET/CT and 68Ga-PSMA-PET/CT studies were interpreted visually and semiquantitatively using the SUVmax values, on a patient-by-patient and lesion-by-lesion basis. In patient-based analysis, detection rate (DR) was defined as the ability to detect at least one pathologic finding in each patient (**Figure 1**).

Statistical methods

The objective of our investigation was to calculate and compare the DRs of the 68Ga-PSMA-PET/CT with the standard imaging 18F-FDG-PET/CT. DRs were calculated as the ratio between the number of positive tumor lesions
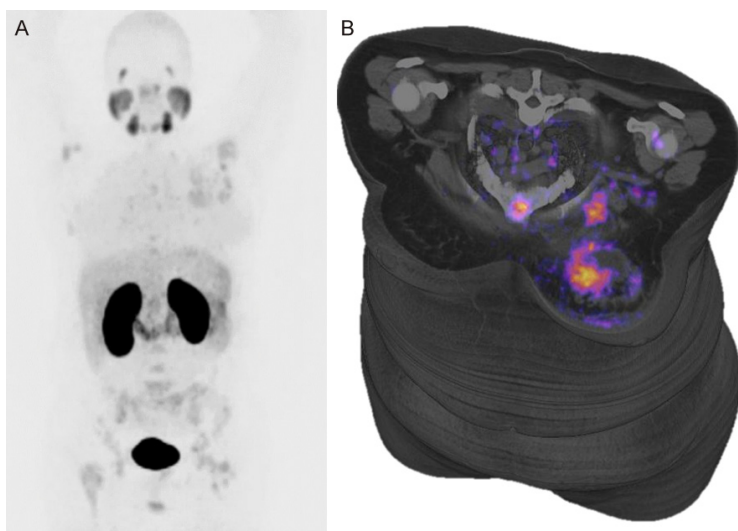
Figure 2. (A) Maximal intensity projection (MIP) Positron Emission Tomography PET with ^{68}Ga-PSMA in patient with LUM-A breast cancer, showed normal biodistribution and primary site in left breast, multiple bone and axillar lymph-node metastases are present; in the left breast are present necrosis in center of tumor (B).

Table 2. Patient-based analysis

Breast cancer subtype	Site lesion	^{18}F-FDG	^{68}Ga-PSMA-11
LUM A	Local	4/4	2/4
	Lymph-node disease	4/4	1/4
	metastatic disease	3/3	2/3
LUM B HER2$^-$	Local	4/4	2/4
	Lymph-node disease	2/2	1/2
	metastatic disease	3/3	3/3
LUM B HER2$^+$	Local	2/2	2/2
	Lymph-node disease	1/1	
	metastatic disease	2/2	2/2
HER-2 overexpression	Local	6/6	5/6
	Lymph-node disease	5/5	
	metastatic disease	4/4	4/4
TPN	Local	5/5	5/5
	Lymph-node disease	5/5	5/5
	metastatic disease	3/3	3/3

Abbreviations: LUM = molecular subtypes of breast cancer including luminal A and luminal B; HER-2 = human epidermal growth factor receptor 2; TPN = triple negative breast cancer.

erating-characteristics (ROC) analysis using MedCalc v.17.1 (MedCalc Software, Ostend, Belgium). A P<0.05 was considered to be statistically significant. Statistical analyses were conducted with software SPSS (version 22).

Results

Patient-based analysis

BC was identified in nearly all patients with ^{18}F-FDG-PET/CT. Local metabolic activity was found in nearly-all patients (99%). We identified lymph node metastases in 17 patients (81%) and metastatic disease was found in 15 patients (71%). The DRs recorded in different subtypes of BC were considered separately (**Figure 2**). **Table 2** summarizes the differences in DR between ^{68}Ga-PSMA-PET/CT and ^{18}F-FDG-PET/CT.

When we considered the differences between the subtypes of BC populations, we found that patients TPN evaluated with ^{68}Ga-PSMA-PET/CT identified a higher number of positive patients than did LUM A.

Tumor-based analysis

To determine the DR of two radiotracers in detecting lesions, we performed a lesion-based analysis; the results are summarized in **Table 3**. A total 127 lesions were detected by ^{18}F-FDG-PET/CT, 30 of which were in the breast, 31 axillary lymph-node metastases, 25 mediastinal lymph-node metastases, 15 distant non-bone metastases and 26 bone metastases. ^{68}Ga-PSMA-PET/CT showed lower DRs than did ^{18}F-FDG-PET/CT in all patients with LUM-A and LUM-B HER2. All ^{18}F-FDG PET/CT positive lesions in patients TPN (local, lymph nodes, and metastatic lesions) showed ^{68}Ga-PSMA-

visualized by ^{68}Ga-PSMA-PET/CT and the total number of tumor lesions visualized by ^{18}F-FDG-PET/CT. The McNemar test was used to compare DRs between both radiotracers on the same patients. SUVmax values between different subtypes were assessed using Student's t test. Sensitivities, specificities and areas under the curve (AUC) were calculated by receiver-op-

Table 3. Tumor-based analysis

Breast cancer subtype	Site lesion	^{18}F-FDG	^{68}Ga-PSMA-11	P*
LUM A	Local	6/6	2/6	0.02
	Axillary lymph-node	4/4	1/4	
	mediastinal lymph-node	3/3	1/3	
	distant non-bone metastases	2/2	1/2	
	bone metastases	4/4	2/4	
LUM B HER2⁻	Local	5/5	3/5	0.05
	Axillary lymph-node	7/7	3/7	
	mediastinal lymph-node	5/5	3/5	
	distant non-bone metastases	4/4	2/4	
	bone metastases	3/3	3/3	
LUM B HER2⁺	Local	8/8	4/8	0.61
	Axillary lymph-node	5/5	3/5	
	mediastinal lymph-node	6/6	5/6	
	distant non-bone metastases	2/2	1/2	
	bone metastases	5/5	5/5	
HER-2 overexpression	Local	6/6	5/6	0.87
	Axillary lymph-node	9/9	8/9	
	mediastinal lymph-node	3/3	3/3	
	distant non-bone metastases	4/4	4/4	
	bone metastases	5/5	5/5	
TPN	Local	5/5	5/5	1.0
	Axillary lymph-node	6/6	6/6	
	mediastinal lymph-node	8/8	8/8	
	distant non-bone metastases	3/3	3/3	
	bone metastases	9/9	9/9	

Abbreviations: LUM = molecular subtypes of breast cancer including luminal A and luminal B; HER-2 = human epidermal growth factor receptor 2; TPN = triple negative breast cancer. *McNemar test vs. ^{68}Ga-PSMA-11 PET/CT.

PET/CT uptake (**Figure 3**). No difference in bone metastases DR was observed between ^{18}F-FDG-PET/CT and ^{68}Ga-PSMA-PET/CT in the different subtypes of BC. The difference between the DR of ^{68}Ga-PSMA-11 PET/CT lesions TPN and HER2 overexpression with lesions by LUM-A was statistically significant (P = 0.02).

This resulted in sensitivities and specificities of 99.2% and 93.6% for ^{18}F-FDG-PET/CT and for ^{68}Ga-PSMA-PET/CT of 84% and 91.8% respectively (**Table 4**), because twenty-seven lesions remained equivocal (P<0.05) in comparison to ^{18}F-FDG-PET/CT), maybe due to maybe more active tumoral cells are better visualized with ^{68}Ga-PSMA due to lower uptake in the associated inflammatory process (see **Figure 3**). Accuracy measured as AUC was 0.86-0.95 in ^{18}F-FDG-PET/CT and 0.74-0.94 for ^{68}Ga-PSMA-PET/CT (P<0.05).

Discussion

PSMA regulates tumor cell invasion and tumor angiogenesis by modulating integrin signal transduction in endothelial cells. The transcription of PSMA can be selectively activated through a transcriptional enhancer region in endothelial cells of the tumor neovasculature, but this region is absent in normal blood vessels [14].

^{68}Ga-PSMA-PET/CT imaging was originally considered to be prostate specific valuable imaging modality for evaluation of primary prostate cancer and it seems to have potential for the detection of lymph node and bone metastases, meanwhile this demonstrated that other tumors have overexpression of this glycoprotein *in-vitro*, and the PET technique can be demonstrated *in-vivo* [15-17].
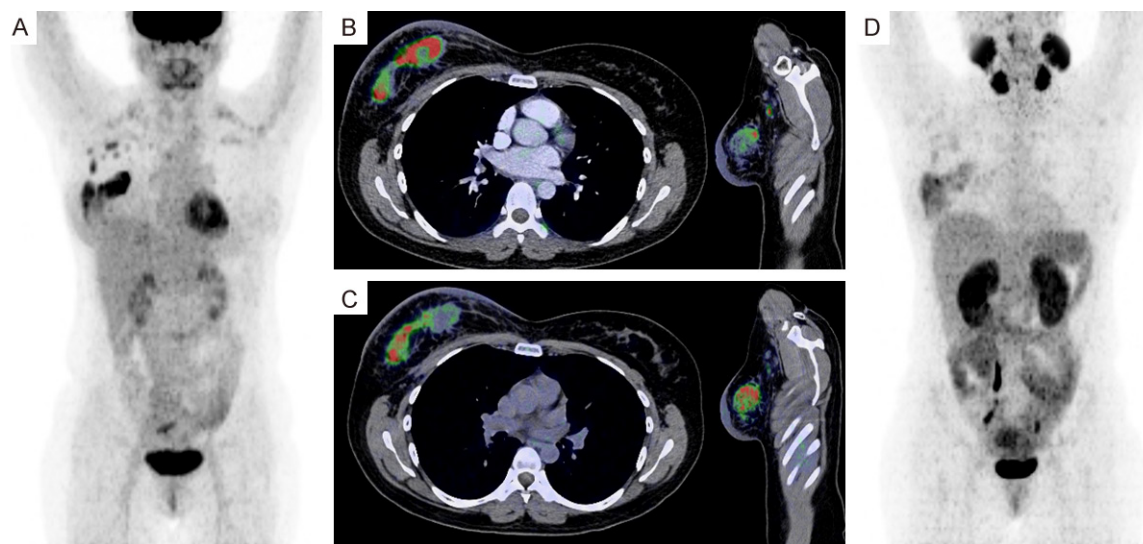
Figure 3. (A) Maximal intensity projection (MIP) Positron Emission Tomography PET with ^{18}F-FDG in patient with TPN breast cancer, showed normal biodistribution and primary site in right breast, and axillary lymph-node metastases; axial and sagittal fused slices showed primary site with non-uniform pattern due to necrosis (B). In the same slices with PET with ^{68}Ga-PSMA the necrosis in the primary site are more pronounced and axillary lymph-node metastases showed uptake (C), and MIP showed similarly pattern (D), maybe more active tumoral cells are better visualized with ^{68}Ga-PSMA due to lower uptake in the associated inflammatory process.

Table 4. Lesion-based analysis of ^{18}F-FDG-PET/CT and ^{68}Ga-PSMA-PET/CT

	PET/CT ^{18}F-FDG	PET/CT ^{68}Ga-PSMA	*p* value
Sensitivity	100 (100)	84.0 (63.9-95.5)	0.044
Specificity	93.6 (88.5-96.6)	91.8 (83.8-96.6)	0.039
AUC	0.91 (0.86-0.95)	0.86 (0.74-0.94)	0.040

Values are percentages in sensitivity and specificity and decimals in AUC and *p*-values. 95% CI are given in parentheses. *P*-values are related to AUC comparison. AUC = Area under the curve. The percentages represent are summarized all molecular subtypes of breast cancer.

To date, our study is the second that has assessed PSMA expression in-vivo in a cohort of patients with primary and metastatic BC. Unlike the previous study conducted by Sathekge M et al. [11], our study did not evaluate recurrence because the objective was to evaluate the locally advanced and metastatic disease from the initial evaluation, and to avoid any possible effect of the oncological therapy used. In addition, our study evaluated DR Patient-Based analysis and Tumor-Based Analysis.

This study demonstrates *in-vivo* PSMA positivity in up to 76% of BC and metastatic disease in more than 90% of patients. Importantly, PSMA tumoral uptake is pronounced in subtype TPN

and HER2 overexpression. Our findings are consistent, in part, with Sathekge results which observed that PSMA SUVmean values was higher metastases when compared to those of primary or local recurrences. Nevertheless, we showed more pronounced uptake in lymph nodes especially in patients TPN and HER2 overexpression in contrast to Sathekge, they report SUVmean values of hormone receptor-positive lesions not significantly different from hormone receptor-negative negative lesions.

We previously report the case of a 45-year-old woman with a single brain metastasis from breast carcinoma HER2 positive seen on ^{68}Ga-PSMA-PET/CT. Biopsy documented disease progression despite treatment [18].

Chang *et al.* [19] were perhaps the first to demonstrate by immunohistochemistry the presence of PSMA in 5 of 6 cases of breast cancer, characterized by the monoclonal antibody 7E11 and those of four recently developed anti-PSMA mAbs (J591, J415, and Hybritech PEQ226.5 and PM2J004.5), each of which binds a distinct epitope of PSMA; this study confirm PSMA expression in the neovasculature of a wide spectrum of malignant neoplasms; rather than a PSMA-like molecule, is

expressed in tumor-associated neovasculature.

Moreover Nguyen et al. [20] studied four external domain-binding anti-PSMA mAbs (J591, J415, J533, and E99) and showed that each bound the tumor-associated neovasculature in several variety of carcinomas (including lung, colon, breast, and others).

Wernicke et al. [9] evaluated a ninety-two patients had primary breast cancer (invasive breast carcinoma with or without co-existing ductal carcinoma in situ (DCIS) or DCIS alone). In addition, 14 patients with breast cancer metastases to the brain. Tumor-associated vasculature was PSMA-positive in 68/92 (74%) of primary breast cancers and in 14/14 (100%) of breast cancers metastatic to brain. PSMA was not detected in normal breast tissue or carcinoma cells.

Tolkach Y et al. [21] they have the most large study in patients with breast cancer evaluate with they have the most large study in patients with breast cancer evaluate PSMA expression on tumor endothelia by immunohistochemistry and mRNA expression of the FOLH1 gene in a large cohort. 315 patients had of invasive carcinoma and lobular breast cancer. Sixty percent of breast cancer cases showed PSMA positivity in tumor vessels with higher expression rates in tumors of higher grade, HER2 overexpression, and lack of positive hormone receptors. These findings were confirmed on mRNA expression levels. The highest PSMA rates were observed in TPN. Nevertheless, they did not use 68Ga-PSMA PET/CT, except in one patient with metastatic breast cancer who underwent PSMA-radionuclide therapy with poor results.

Another study development by Kasoha M et al. [22] evaluated by immunohistochemical analysis that primary breast tumors and distant metastases showed PSMA expression in tumor cells and in tumor associated neovasculature. In addition, distant metastases showed higher PSMA expression in tumor-associated neovasculature comparing with primary tumors associated with histologic type and tumor grade with statistical significance.

Some important limitations should be observed. First, we assessed only the DRs of the 68Ga-PSMA PET/CT, assuming a priori that all patients were true-positives, we not performed immunohistochemical analysis for evaluate PSMA expression. This study is limited by its retrospective study design. Histological proof was not available as reference standard to determine the true dignity of bone metastases. Another potential limitation was our limited number of patients by subtypes of BC, so we decided to evaluate the DRs based on the Tumor-Based Analysis.

Conclusion

Our study showed a significate DRs to PET imaging with 68Ga-PSMA in the staging of locally advanced and metastatic BC with high rates in patients TPN LUM B HER2+ and HER2 overexpression. We believe that concept of theranostics it may be considered as a potential diagnostic and therapeutic target. Based in this findings larger trials are necessary to further define the role according the subtype of BC.

Acknowledgements

We thank Breast Tumors and Nuclear Medicine Department at Instituto Nacional de Cancerologia, México.

Disclosure of conflict of interest

None.

Address correspondence to: Sevastian Medina-Ornelas, Department of Nuclear Medicine and Molecular Imaging, Instituto Nacional de Cancerología, México. Sevastián S. Medina Ornelas. Av. San Fernando, 22 Col. Sección XVI, Del. Tlalpan, C.P. 14080, Ciudad de México, México. Tel: 0155 47471027 Ext. 10115; E-mail: dr.sevastian@outlook.com

References

[1] GLOBOCAN 2018 v1.0, Cancer Incidence and Mortality Worldwide: IARC Cancer Base No. 11 [Internet]. Lyon, France: International Agency for Research on Cancer. Available from: http://www.gco.iarc.fr/today/datasources-methods. accessed on 20/Jun/2019.

[2] Siegel RL, Miller KD and Jemal A. Cancer statistics CA Cancer. J Clin 2017; 67: 7-30.

[3] Mariotto AB, Etzioni R, Hurlbert M, Penberthy L and Mayer M. Estimation of the number of women living with metastatic breast cancer in the United States. Cancer Epidemiol Biomarkers Prev 2017; 26: 809-815.

[4] Lebron L, Greenspan D and Pandit-Taskar N. Pet imaging of breast cancer: role in patient management. PET Clin 2015; 10: 159-95.

[5] Breast cancer. In National Comprehensive Cancer Network (NCCN) Clinical Practice Guidelines in Oncology, version 1.2020. National Comprehensive Cancer Network. accessed on 16/february/2020.

[6] Silver DA, Pellicer I, Fair WR, Heston WD and Cordon-Cardo C. Prostate-specific membrane antigen expression in normal and malignant human tissues. Clin Cancer Res 1997; 3: 81-85.

[7] Mhawech-Fauceglia P, Zhang S, Terracciano L, Sauter G, Chadhuri A, Herrmann FR and Penetrante R. Prostate-specific membrane antigen (PSMA) protein expression in normal and neoplastic tissues and its sensitivity and specificity in prostate adenocarcinoma: an immunohistochemical study using mutiple tumour tissue microarray technique. Histopathology 2007; 50: 472-483.

[8] Kinoshita Y, Kuratsukuri K, Landas S, Imaida K, Rovito PM, Wang CY and Haas GP. Expression of prostate-specific membrane antigen in normal and malignant human tissues. World J Surg 2006; 30: 628-636.

[9] Wernicke AG, Varma S, Greenwood EA, Christos PJ, Chao KS, Liu H, Bander NH and Shin SJ. Prostate-specific membrane antigen expression in tumor-associated vasculature of breast cancers. APMIS 2014; 122: 482-489.

[10] Nomura N, Pastorino S, Jiang P, Lambert G, Crawford JR, Gymnopoulos M, Piccioni D, Juarez T, Pingle SC, Makale M and Kesari S. Prostate specific membrane antigen (PSMA) expression in primary gliomas and breast cancer brain metastases. Cancer Cell Int 2014; 14: 26.

[11] Sathekge M, Lengana T, Modiselle M, Vorster M, Zeevaart JR, Maes A, Ebenhan T and Van de Wiele C. 68Ga-PSMA-HBEDCC PET imaging in breast carcinoma patients. Eur J Nucl Med Mol Imaging 2017; 44: 689-694

[12] Sawicki LM, Buchbender C, Boos J, Giessing M, Ermert J, Antke C, Antoch G and Hautzel H. Diagnostic potential of PET/CT using a 68 Ga-labelled prostate-specific membrane antigen ligand in whole-body staging of renal cell carcinoma: initial experience. Eur J Nucl Med Mol Imaging 2017; 44: 102-107.

[13] Hangaard L, Jochumsen MR, Vendelbo MH and Bouchelouche K. Metastases from colorectal cancer avid on 68 Ga-PSMA PET/CT. Clin Nucl Med 2017; 42: 532-533.

[14] Conway RE, Petrovic N, Li Z, Heston W, Wu D and Shapiro LH. Prostate-specific membrane antigen regulates angiogenesis by modulating integrin signal transduction. Mol Cell Biol 2006; 26: 5310-5324.

[15] Medina-Ornelas SS, García-Pérez FO, Hernández-Pedro N, Arellano-Zarate A and Abúndiz-López B. Correlation between molecular tumor volume evaluate with 68Ga-PSMA PET/CT and antigen prostatic specific levels. Rev Esp Med Nucl Imagen Mol 2018; 37: 223-228.

[16] Afshar-Oromieh A, Zechmann CM, Malcher A, Eder M, Eisenhut M, Linhart HG, Holland-Letz T, Hadaschik BA, Giesel FL, Debus J and Haberkorn U. Comparison of PET imaging with a (68) Ga-labelled PSMA ligand and (18)F-choline-based PET/CT for the diagnosis of recurrent prostate cancer. Eur J Nucl Med Mol Imaging 2014; 41: 11-20.

[17] Afshar-Oromieh A, Avtzi E, Giesel FL, Holland-Letz T, Linhart HG, Eder M, Eisenhut M, Boxler S, Hadaschik BA, Kratochwil C, Weichert W, Kopka K, Debus J and Haberkorn U. The diagnostic value of PET/CT imaging with the (68) Ga-labelled PSMA ligandHBED-CC in the diagnosis of recurrent prostate cancer. Eur J Nucl Med Mol Imaging 2015; 42: 197-209.

[18] Medina-Ornelas SS, García-Pérez FO, Medel-Gamez C and Paredes-Amoroto E. A single brain metastasis seen on 68Ga-PSMA PET/CT in recurrent breast cancer. Rev Esp Med Nucl Imagen Mol 2018; 37: 61-62.

[19] Chang SS, Reuter VE, Heston WD, Bander NH, Grauer LS and Gaudin PB. Five different anti-prostate-specific membrane antigen (PSMA) antibodies confirm PSMA expression in tumor-associated neovasculature. Cancer Res 1999; 59: 3192-3198.

[20] Nguyen DP, Xiong PL, Liu H, Pan S, Leconet W, Navarro V, Guo M, Moy J, Kim S, Ramirez-Fort MK, Batra JS and Bander NH. Induction of PSMA and internalization of an Anti-PSMA mAb in the vascular compartment. Mol Cancer Res 2016; 14: 1045-1053.

[21] Tolkach Y, Gevensleben H, Bundschuh R, Koyun A, Huber D, Kehrer C, Hecking T, Keyver-Paik MD, Kaiser C, Ahmadzadehfar H, Essler M, Kuhn W and Kristiansen G. Prostate-specific membrane antigen in breast cancer: a comprehensive evaluation of expression and a case report of radionuclide therapy. Breast Cancer Res Treat 2018; 169: 447-455.

[22] Kasoha M, Unger C, Solomayer EF, Bohle RM, Zaharia C, Khreich F, Wagenpfeil S and Juhasz-Böss I. Prostate-specific membrane antigen (PSMA) expression in breast cancer and its metastases. Clin Exp Metastasis 2017; 34: 479-490.